SCIENTIFIC REPORTS

OPEN

SUBJECT AREAS:
PRECLINICAL RESEARCH
BIOMEDICAL MATERIALS

Received
9 June 2014

Accepted
15 October 2014

Published
5 November 2014

Correspondence and requests for materials should be addressed to X.B. (baixc15@smu.edu.cn); J.Y. (jxy30@psu.edu) or D.J. (wmyqxqj@gmail.com)

* These authors contributed equally to this work.

Citric Acid-based Hydroxyapatite Composite Scaffolds Enhance Calvarial Regeneration

Dawei Sun[1,2]*, Yuhui Chen[1]*, Richard T. Tran[3]*, Song Xu[1,4], Denghui Xie[1,3], Chunhong Jia[4], Yuchen Wang[1], Ying Guo[1], Zhongmin Zhang[1], Jinshan Guo[3], Jian Yang[3], Dadi Jin[1] & Xiaochun Bai[1,4]

[1]Academy of Orthopedics, Guangdong Province, Department of Orthopedics, The Third Affiliated Hospital, Southern Medical University, Guangzhou, 510665, China, [2]Department of Orthopaedics & Microsurgery, Guangdong No. 2 Provincial People's Hospital, Guangzhou, 510317, China, [3]Department of Biomedical Engineering, Materials Research Institute, The Huck Institutes of The Life Sciences, The Pennsylvania State University, University Park, Pennsylvania, 16802, U.S.A, [4]State Key Laboratory of Organ Failure Research, Department of Cell Biology, School of Basic Medical Science, Southern Medical University, Guangzhou, 510515, China.

Citric acid-based polymer/hydroxyapatite composites (CABP-HAs) are a novel class of biomimetic composites that have recently attracted significant attention in tissue engineering. The objective of this study was to compare the efficacy of using two different CABP-HAs, poly (1,8-octanediol citrate)-click-HA (POC-Click-HA) and crosslinked urethane-doped polyester-HA (CUPE-HA) as an alternative to autologous tissue grafts in the repair of skeletal defects. CABP-HA disc-shaped scaffolds (65 wt.-% HA with 70% porosity) were used as bare implants without the addition of growth factors or cells to renovate 4 mm diameter rat calvarial defects (n = 72, n = 18 per group). Defects were either left empty (negative control group), or treated with CUPE-HA scaffolds, POC-Click-HA scaffolds, or autologous bone grafts (AB group). Radiological and histological data showed a significant enhancement of osteogenesis in defects treated with CUPE-HA scaffolds when compared to POC-Click-HA scaffolds. Both, POC-Click-HA and CUPE-HA scaffolds, resulted in enhanced bone mineral density, trabecular thickness, and angiogenesis when compared to the control groups at 1, 3, and 6 months post-trauma. These results show the potential of CABP-HA bare implants as biocompatible, osteogenic, and off-shelf-available options in the repair of orthopedic defects.

Over 2.2 million bone transplantation procedures are performed annually worldwide in a variety of fields including orthopedics, neurosurgery, and dentistry[1]. Although, autologous bone grafts remain the gold standard for bone grafting procedures due to their superior osteogenic potential, their use is associated with various complications such as hematoma, soft tissue breakdown, pain, and prolonged recovery times[2,3]. Moreover, the use of bone autografts is contraindicated in osteoporotic populations due to a significant reduction in bone quality and quantity[4]. Thus, the development of a fully synthetic, readily available, and osteogenic bone substitute as an adjunct to autologous tissue grafts is strongly encouraged and considered as a great milestone in the clinical field.

For synthetic orthopedic biomaterials, research in the field has witnessed a shift from the use of permanent, inert metals towards tissue-engineered biodegradable composites designed to mimic the native composition of bone. Initially, the majority of synthetic orthopedic materials were based off calcium phosphates (CaPs), such as hydroxyapatite (HA) and beta tricalcium phosphate (TCP), because of their ability to replicate the native mineral constituent of bone tissue[5–9]. Although biomimetic and osteogenic, their applications are severely limited when fabricated into porous structures due to the inherent brittleness and very slow degradation rates[10–12]. To improve their utility, the hybridization of bioceramics and biodegradable polymers has been widely adopted to reform the mechanical properties and bioactivity of the resulting materials for orthopedic applications[13]. However, the current composite materials still suffer from several significant problems such as unsatisfactory mechanical strength, inefficient bone regeneration, poor bone integration, and the inability to mimic native bone chemical composition, which is composed of 60–65 wt.-% hydroxyapatite embedded in a collagen matrix[14,15].

To address these limitations, our lab has focused on the development of citric acid-based materials to composite with bioceramics for orthopedic tissue engineering. Citrate, a naturally occurring Kreb's cycle product, is

highly conserved in native bone with over 90% of the body's total citrate content being located in the skeletal system. Recent research has suggested that citrate plays significant roles in bone anatomy, physiology, and orthopedic biomaterial development[16–18]. For example, citrate is not only a dissolved calcium-solubilizing agent, but has recently been found to be an integral part of the bone nanocomposite. Previous research by Hu *et al.* and Davies *et al.* has shown that citrate molecules are strongly studded to the apatite nanocrystal surface and form bridges between mineral platelets regulating bone mineral crystallinity, respectively, which is highly related to the overall strength of bone tissue[16,19]. Along with the recent exciting and significant strides that have been made elucidating the role of citrate in bone formation and physiology, our lab has recently shown the potential of citrate as a cornerstone in orthopedic biomaterial design. Our recent exciting results showed that exogenous citrate, whether presented on a biomaterial, supplemented into culture media, or released from a biomaterial over the course of degradation can enhance alkaline phosphatase (ALP) and osterix (OSX) gene expression, osteoblast phenotype progression, implant osteoinductivity, and osteointegration both *in vitro* and *in vivo*[17]. The natural abundance of citrate in bone tissue, its importance in bone physiology, and our recent findings on stem cell culture hint that citrate may have significant impacts on bone development and orthopedic biomaterial development[19,20].

As previously mentioned, citric acid-based polymer/hydroxyapatite composites (CABP-HAs) are a novel class of orthopedic biomaterial, which offer distinct advantages for bone tissue engineering applications[17]. The first reported citric acid-based composite, poly (1,8-octanediol)-HA (POC-HA), is synthesized with non-toxic monomers using simple and cost-effective procedures. POC-HA displayed enhanced HA integration through the calcium chelating ability of free carboxylic chemistry in the bulk of the material[20]. The abundant carboxyl chemistry allowed for the incorporation of up to 65 wt.-% of HA in the composites to match the native mineral content of bone tissue and is a feature that is not possible with previous materials. Since the development of POC-HA, our laboratory has long been working on a series of citrate-based biodegradable polymers such as mechanically strong crosslinked urethane-doped polyesters (CUPEs)[21], biodegradable photoluminescent polymers (BPLPs)[22,23], dual-crosslinkable poly (alkylene maleate citrate) (PAMC)[24,25], and clickable POC-based elastomers (POC-Click)[26] for various biomedical applications such as bone, vascular, and neural tissue engineering, cancer imaging, and drug delivery[17,27–29]. To improve upon the mechanical properties of POC-HA through urethane chemistry, we have shown that CUPE-HA composites display impressive compressive strengths of 116.23 ± 65.37 MPa, which falls within the range of native human cortical bone (100–230 MPa). Although, CUPE-HA showed minimal chronic inflammation and full osteointegration when implanted in a rabbit lateral femoral condyle defect model, the urethane-doping strategy sacrificed valuable pendant carboxyl chemistry to chelate with hydroxyapatite limiting the mechanical potential of the material[17,21,24].

To address this situation, we have recently developed a clickable biodegradable elastomer, poly (octanediol citrate) – click (POC-Click), which employs azide-alkyne cycloaddition (click chemistry) as an additional crosslinking mechanism to improve the mechanical strength of the bulk material without sacrificing valuable pendant citric acid carboxyl chemistry for HA calcium chelation[26]. Although we have previously shown that citrate-based materials can address the challenges in designing mechanically strong, osteoconductive, and osteoinductive orthopedic biomaterials, this new class of orthopedic biomaterials has only been studied as solid, non-porous implants, and their use as a scaffold for cranial bone defect repair has not been studied yet. Therefore, in this study, CUPE-HA and POC-Click-HA porous scaffolds were fabricated and compared for their potential to repair cranial defects in rats.

Methods

Hydroxyapatite [Mw: 502.32, assay > 90% (as $Ca_3(PO_4)_2$); particle size: > 75 μm (0.5%), 45–75 μm (1.4%), < 45 μm (98.1%)] and all remaining chemicals were purchased from Sigma-Aldrich (St. Louis, MO, USA) and used as received unless stated otherwise.

Scaffold fabrication. CUPE pre-polymers and POC-Click (clickable diols 30% of total diol composition) pre-polymers were synthesized according to previously published methods[21,26]. To fabricate porous CUPE-HA disc shaped scaffolds, CUPE pre-polymer was first dissolved in 1,4-dioxane and mixed with hydroxyapatite (65 wt.-%). Next, sodium chloride salt with an average size in the range of 200–400 μm was added to the mixture (70 wt.-%) and stirred in a Teflon dish until a homogenous viscous paste was formed. To fabricate disc-shaped scaffolds, the viscous paste was inserted into Teflon tubes (4 × 2 mm; inner diameter × height) purchased from McMaster-Carr (Aurora, OH, USA). Following solvent evaporation, the scaffolds were post-polymerized in an oven maintained at 100°C for 3 days. Salt was leached out from the scaffolds by immersion in deionized water under vacuum for 72 hours with water changes every 12 hours. Finally, the scaffolds were dried using lyophilization to obtain the final disc-shaped scaffolds (4 × 2 mm; diameter × height). POC-Click-HA disc shaped scaffolds were also fabricated as described above.

Ethics Statement. All animal experiments were carried out with the approval of the Southern Medical University Animal Care and Use Committee in accordance with the guidelines for the ethical treatment of animals. All surgeries were performed under chloral hydrate and xylazine anesthesia, and all efforts were made to minimize animal suffering.

Surgical procedure. Seventy-two male Sprague–Dawley rats (200–220 g) were used for the animal experiments. The body weights were closely monitored to confirm feeding and expected growth rates. All rats were handled regularly for at least one week prior to surgery and individually housed in cages in climate controlled rooms at 22°C with 50% humidity and 12 h light/dark cycles. Surgeries were performed under semi-sterile conditions with animals under anesthesia induced by the intraperitoneal injection of 100 mg/kg chloral hydrate and 10 mg/kg xylazine. The surgical site was shaved and prepared with a 70% ethanol solution, and a subcutaneous injection of 0.5 mL of 1% lidocaine (local anesthetic) was given at the sagittal midline of the skull. Following this injection, a sagittal incision was made over the scalp from the nasal bone to the middle sagittal crest, and the periosteum was bluntly dissected. Using a punch, a 4 mm diameter pit defect was made with a trephine drill, which was constantly cooled with sterile saline. The calvarial disk was then carefully removed to avoid tearing of the dura. Animals were randomly assigned into four groups (n=18 per group) in which the 4 mm defect was: 1) left empty as a negative control (CON), 2) filled with autogenous bone (AB), 3) filled with CUPE-HA scaffolds (CUPE-HA), or 4) filled with POC-Click-HA scaffolds (POC-Click-HA). The skin was sutured with 6-0 vicryl, and the animals were monitored following standard post-operative animal care protocols (Fig. S1). Animals were ultimately anesthetized and sacrificed by xylazine injection at 1, 3, 6 months post-surgery.

Scanning electron microscope. Bare CABP-HA scaffolds and explanted scaffolds isolated 6 months after surgery were fixed with 2.5% glutaraldehyde (Sigma, USA) for 12 h and characterized using scanning electron microscopy (SEM). After tension-free drying, the samples were coated in gold and analyzed with a S-3000N SEM (Hitachi, Japan) under high-vacuum conditions (air pressure$<1 \times 10^{-7}$ mbar), 20 kV voltage, and 18 mm working distance. A Philips XL 30 ESEM-FEG system (FEI Co, USA) was used to capture images at 50× and 500× magnification.

Microcomputed tomography (micro CT). Micro CT analysis was used to quantify the volume of bone formation within the defect. The tomography of fixed rat calvarial bone specimens was performed using a microtomographic imaging system (ZKKS-MCT-Sharp-III scanner, Caskaishen, China) at 50 kV, 40 W, and an exposure time of 300 ms through a 0.5-mm-thick aluminum filter. The X-ray projections were obtained at 0.72° intervals with a scanning angular rotation of 360°. The reconstructed dataset was segmented by an automated thresholding algorithm. The projection images were reconstructed into three-dimensional images using ZKKS-MicroCT software (version 4.1) from ZKKS. To calculate the bone mineral density (BMD) and trabecular thickness (Tb.Th) among the four groups, a hollow cylindrical volume of interest (VOI-1) 4 mm in external diameter, 2.8 mm in inner diameter, and 300 μm in height was selected for scanning and corrected for the CT value to evaluate the bone regeneration at the periphery of the implant areas (Fig. 1A). To further evaluate bone regeneration between the CUPE-HA and POC-Click-HA groups in the entire defect areas, a cylindrical volume of interest (VOI-2) 4 mm in diameter and 300 μm in height was selected to analyze the BMD and Tb.Th (Fig. 1B).

Histological assessment. For histological assessment, the defect and surrounding tissues were fixed in 4% paraformaldehyde for 48 h, decalcified with 0.5 M ethylenediaminetetraacetic acid (EDTA) at pH 7.4 for 3 weeks, and embedded in paraffin. Tissues were longitudinally sectioned with a 4-μm thickness, deparaffinated with xylene, gradually hydrated, and stained with hematoxylin and eosin (H&E) for light microscopic analysis. Images were captured at 200× magnification using an Olympus bx51 microscope with a 20× objective lens (Olympus, Japan) and a digital camera (ProgRes C14, Jenoptik, Germany). Five random images were obtained for each rat along the length of the defect. Overall, a total of 25 to 30 images were acquired

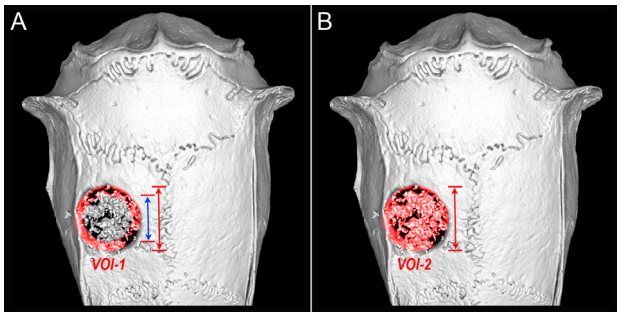

Figure 1 | Representative image depicting the anatomical region used to define the volume of interest (VOI) used for bone mineral density (BMD) and trabecular thickness (Tb.Th) measurements in axial view. A) A hollow VOI-1 (red circular area) was defined as the space between outer circle (4 mm in diameter; red arrow) and inner circle (2.8 mm in diameter; blue arrow) with a depth of 300 μm to measure mineralized tissue at the periphery of the implant, and B) a solid cylindrical VOI-2 (red circular area) was defined as the entire defect area (4 mm in diameter; red arrow) with a depth of 300 μm.

from five to six rats in each group. The number of blood vessels was determined by counting luminal structures lined by vascular endothelium and partially filled with red blood cells[30]. The deparaffinated slices were stained using Alkaline Phosphatase Kit based on naphthol AS-MX phosphate and fast blue RR salt (Sigma, MO, USA). Images were observed at 400× magnification.

Immunohistochemical analysis. To stain for osteocalcin (OCN) and Vascular Endothelial Growth Factor-b (VEGF-b), tissue sections were treated with proteinase K (Sigma, MO, USA) for antigen recovery, washed with PBS, blocked with 5% bovine serum albumin at room temperature for 30 min, and exposed to antibodies for VEGF-b (1 : 100 dilution, Bioworld, CA, USA) and osteocalcin (1 : 100 dilution, Santa Cruz, CA, USA) overnight at 4°C. Peroxidase activity was detected using the enzyme substrate 3-amino-9-ethyl carbazole. For negative controls, sections were treated in an identical manner, except they were incubated in PBS-buffered saline without primary antibodies. Vascular numbers were determined by three single blind pathologists and calculated according to the average number of vessels in five random areas of an image at 200× magnification.

Statistical analysis. Data are expressed as the mean ± standard deviation. The statistical significance between two sets of data was calculated using a two-tail Student's t-test. Analysis of variance (ANOVA) with Newman-Keuls multiple comparisons test post-hoc analysis was used to determine significant differences among three or more groups. Data analysis was performed using SPSS 20.0 software. Data were considered to be significant when a p-value of 0.05 or less was obtained.

Results

SEM analysis of CABP-HA scaffolds. SEM images of the disc-shaped CUPE-HA and POC-Click-HA scaffolds fabricated in this study are shown in Figure 2. As shown in the SEM images (Fig 2A-B), a porous structure with an average pore size in the range of 200–400 μm can be seen. The SEM images suggest that the scaffolds present rough pore walls, which may facilitate protein adsorption and cell adhesion. Explanted samples after 6 months of implantation were also viewed under SEM (Fig. 2C–D). As seen from the two SEM images, the overall morphology between the explanted CUPE-HA and POC-Click-HA groups were similar in appearance with dense tissue filling the scaffold pore structures.

Radiographic assessment of new bone formation. To observe new bone formation within the defects, 3D images of the defects were reconstructed using micro-CT 1, 3, and 6 months post-surgery (Fig. 3). Radiographic evidence of new bone formation was highly variable between non-scaffold groups (CON and AB groups) and CABP-HA scaffold groups (CUPE-HA and POC-Click-HA groups). In the untreated defects (CON group), no new bone formation was observed in the defect 6 months after surgery (Figs. 3A–C). In contrast, dense tissue was evident inside the defect of autologous bone treated animals (Figs. 3D–F). In two scaffold groups, radiopaque tissue was found spread over the entire defect site indicating new bone formation. The amount of radiopaque tissue appeared higher in the defects treated with CUPE-HA scaffolds (Figs. 3G–I) compared to POC-Click-HA scaffolds (Figs. 3J–L).

Next, micro-CT analysis was conducted to quantify the mineralized skeletal bone formation at the periphery of the implant using a hollow cylindrical volume of interest (VOI-1) (Fig. 4A and 4B). The highest level of peripheral bone formation was observed in defects

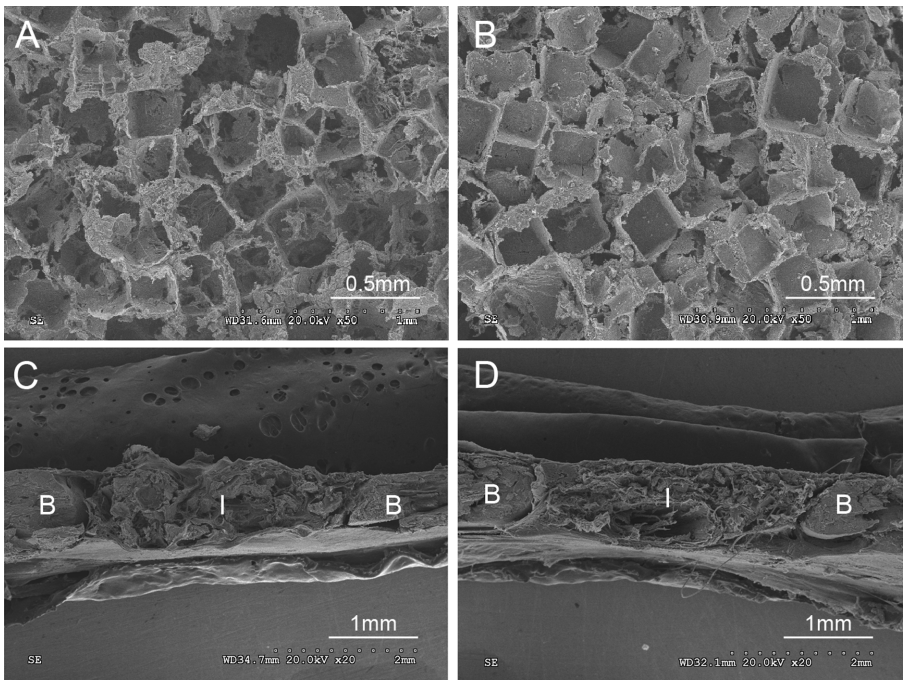

Figure 2 | Representative scanning electron microscope (SEM) images of bare crosslinked urethane-doped polyester – hydroxyapatite (CUPE-HA) scaffolds (A) and (B) poly (octanediol citrate) – click – hydroxyapatite (POC-Click-HA) scaffolds (60 wt.-HA and 70% porosity); and C) CUPE explants and D) POC-click-HA explants 6 months after implantation in a 4 mm rat calvarial defect (magnification 50×) (I: implant; B: bone).

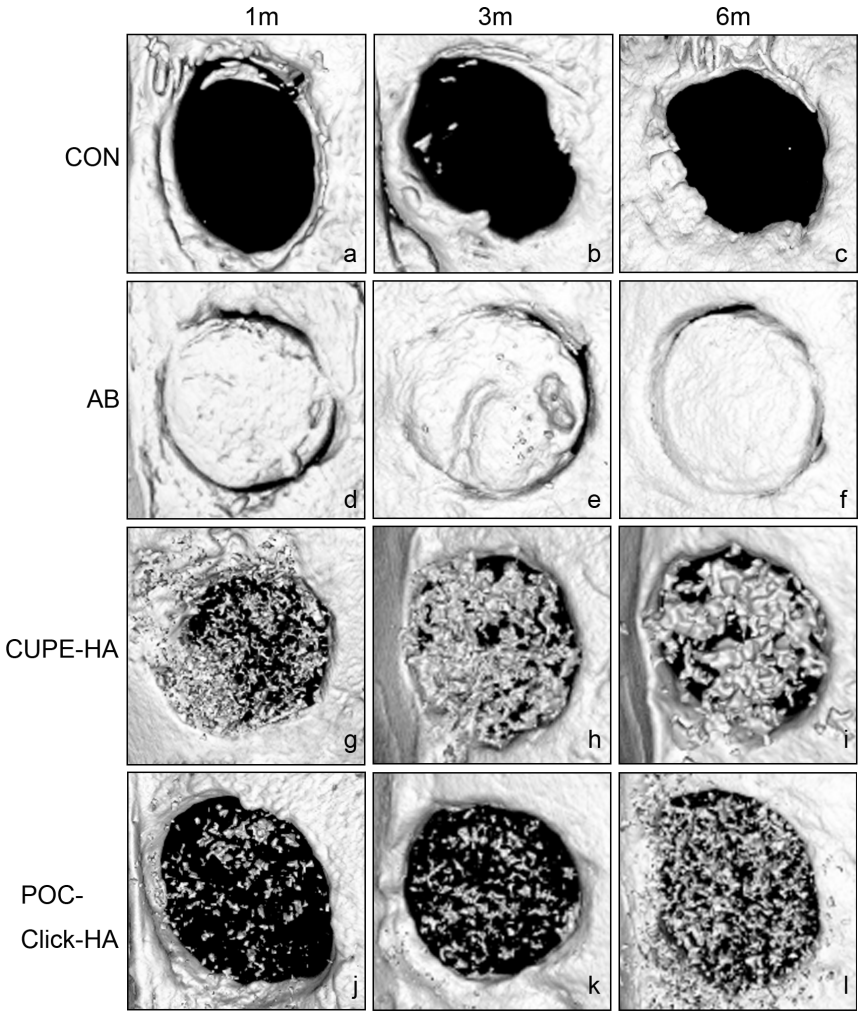

Figure 3 | Microcomputer tomography (micro CT) reconstructed 3D images of 4 mm rat calvarial defects treated with a–c) negative control (untreated defects) (CON), d–f) autologous bone (AB), g–i) crosslinked urethane-doped polyester-hydroxyapatite scaffolds (CUPE-HA), and j–l) poly (octanediol citrate)-click-hydroxyapatite scaffolds (POC-Click-HA) 1, 3, and 6 months post-implantation.

treated with AB compared to all other groups. However, compared to the negative control (CON), the defects repaired with CABP-HA scaffolds exhibited greater peripheral bone regeneration. The peripheral BMD and Tb.Th of the AB group was significantly higher than that of the other groups at 1, 3, and 6 months after surgery ($p<0.001$), which is evidenced by the radiopaque tissue bridging the implant and surrounding bone. The peripheral BMD and Tb.Th of the CUPE-HA and POC-Click-HA groups was significantly higher than the CON group at all time points (Fig. 4A and B) ($p<0.01$). The peripheral BMD and Tb.Th observed between the CUPE-HA group and the POC-Click-HA groups showed no significant difference at all time points ($p>0.05$). To quantify the amount of mineralized tissue within the scaffold treated defect sites, the BMD and Tb.Th was calculated using a solid cylindrical VOI-2 (Fig. 1B). As shown in Figures 4C and D, no significant difference was seen at the 1 month time point for both BMD and Tb.Th (Fig. 4C and 4D, respectively). However, the CUPE-HA treated cranial defects exhibited increased dense tissue formation within the defect sites when compared to the POC-Click-HA group with the higher BMD (*$p<0.05$, **$p<0.01$) (Fig. 4C) and Tb.Th (**$p<0.01$) (Fig. 4D) at 3 and 6 months post-implantation.

Histological assessment. Histological assessment of defect sites in the CUPE-HA and POC-Click-HA groups were similar to the findings in the autologous bone treated group (AB group). Specifically, the edge of the defect site was composed of fibrous stroma and reactive bone. The fibrous stroma appeared loose around the scaffolds and exhibited a relatively high level of angiogenesis. In contrast, the defect sites in the negative control group (CON group) did not exhibit reactive bone formation and displayed less fibrous stroma compared to both the AB and CABP-HA scaffold groups (Fig. 5). Tissue sections were stained for alkaline phosphatase (ALP) to indicate the presence of osteoblast within the defect site 1, 3, and 6 months post implantation (Fig. 6A). Staining for osteocalcin (OCN) was also performed and revealed OCN positive cells in the defect site and were distributed within the implanted scaffolds 1, 3, and 6 months post implantation (Fig. 6B). ALP and OCN positive cells were also quantified in the defect site of AB and CON control group (Fig. S2ab). Immunohistochemical staining for VEGF-b was also performed after 1, 3, and 6 months of implantation (Fig. 7). In the negative control group (without any material implantation), very few fibroblasts and inflammatory cells were concentrated in the defect space and lower levels of VEGF-b expression were observed when compared to the same area of other groups. In contrast, CUPE-HA and POC-Click-HA treated groups showed higher levels of VEGF-b expression and was similar to that of AB group, especially at the 1 month time point (Fig. 7). Quantification of the vessel numbers found in defect sites after 1, 3, and 6 months for all experimental groups are shown in Figure 8. Greater vessel numbers in CABP-HA scaffold treated defects were confirmed by morphometric analysis of the vessels (Fig. 8). The vascular numbers of

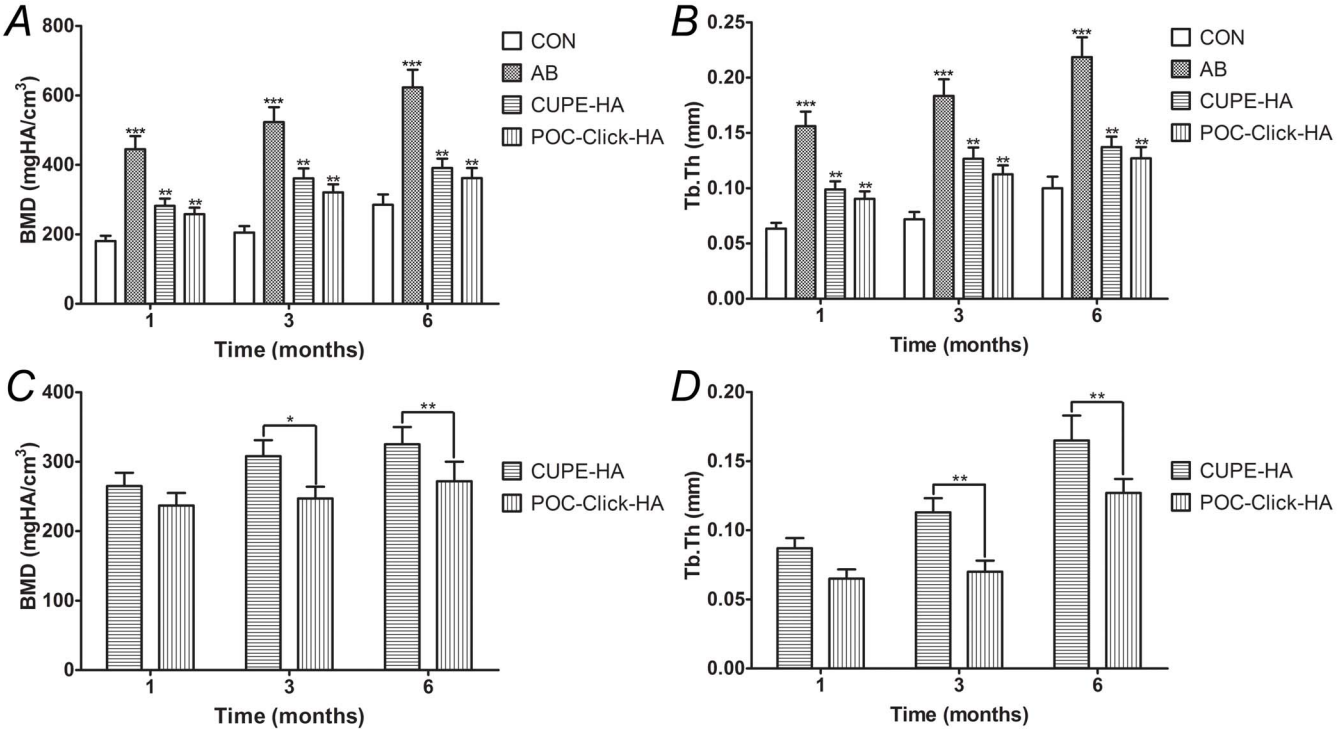

Figure 4 | Morphometric analysis of A and C) bone mineral density (BMD) and B and D) trabecular thickness (Tb.Th) in 4 mm rat calvarial defects after 1, 3, and 6 months of implantation Data are presented as mean ± SD ($n = 3$) (*p<0.05, **p<0.01, ***p<0.001). CON: negative control group; AB: autologous bone group; CUPE-HA: crosslinked urethane-doped polyester-hydroxyapatite composite scaffold treated group; POC-Click-HA: poly (octanediol citrate)-click-hydroxyapatite composite scaffold treated group.

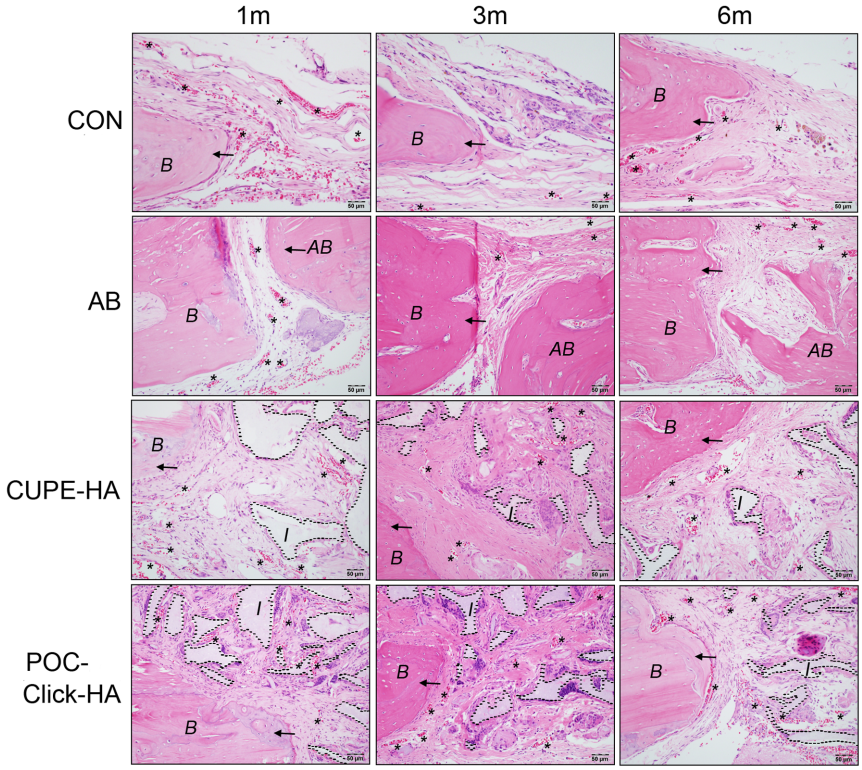

Figure 5 | Microscopic images of hematoxylin and eosin (H&E) stained tissue sections from 4 mm rat calvarial defects after 1, 3, and 6 months of implantation. New bone (arrows) and blood vessel formation (asterisks) were presented in the crosslinked urethane-doped polyester-hydroxyapatite composite scaffold (CUPE-HA) and poly (octanediol citrate)-click-hydroxyapatite composite scaffold (POC-Click-HA) treated animals after 3 and 6 months (magnification 200×). CON: control group; AB: autologous bone group (autogenous bone implant); 1 m, 3 m, and 6 m: 1, 3, and 6 months post-surgery, respectively; I: implant (black dotted lines); B: bone; Arrow: new bone; Asterisks: blood vessel.

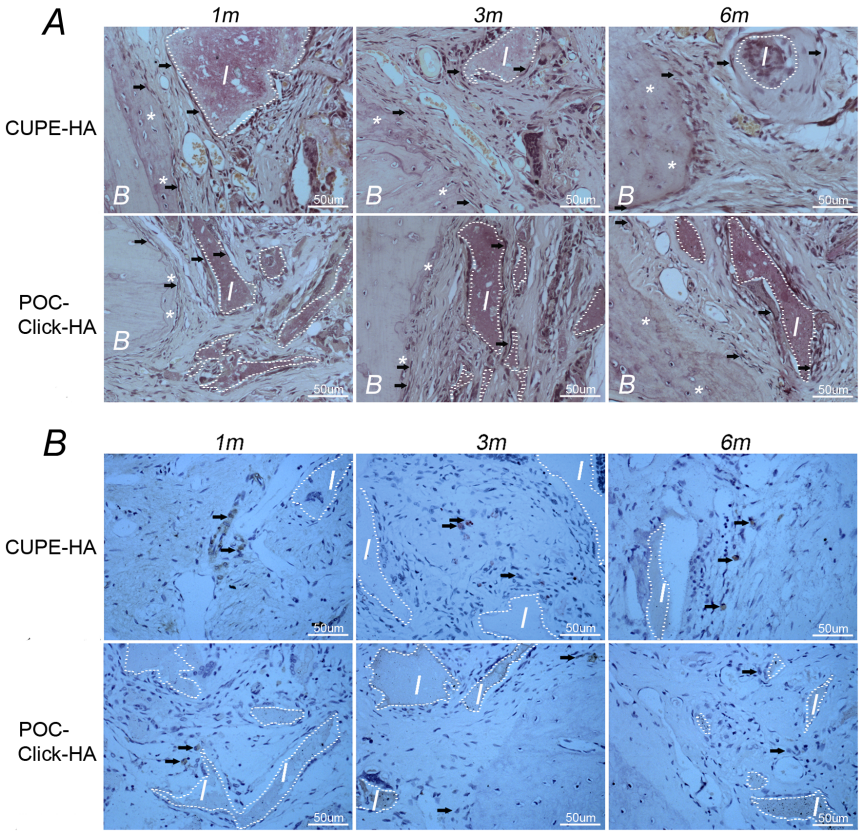

Figure 6 | A) Alkaline phosphatase (ALP) and B) osteocalcin (OCN) specific stained tissue sections from 4 mm rat calvarial defects treated with crosslinked urethane-doped polyester-hydroxyapatite composite scaffolds (CUPE-HA) and poly (octanediol citrate)-click-hydroxyapatite composite scaffolds (POC-Click-HA) 1, 3, and 6 months after surgery. Magnification: 400×; Arrow: ALP-positive (dark brown) or OCN-positive (brown) osteoblasts; I: implant (white dotted lines); B: bone.

CUPE-HA groups were significantly higher than the AB and POC-Click-HA groups 1 month post-surgery ($p<0.05$) (Fig. 8). No significant difference was observed in vascular numbers between each group at 3 and 6 months post-surgery ($p<0.05$).

Discussion

In the early 1960s, it was found that citrate made up about 5 wt.-% of the organic component in bone. Recent studies have found that the surface of apatite nanocrystals is actually strongly bound with citrate molecules, which regulate and stabilize the crystallinity of apatite nanocrystals by bridging mineral platelets[16,19,31]. Our recent reports on citrate-based polymer blend composites have shown that citrate, whether presented on the biomaterial or exogenously supplemented into culture media, can promote bone development through the up regulation of alkaline phosphatase (ALP) and osterix (OSX) gene expression and acceleration of osteoblast phenotype progression[17]. These recent insights have reintroduced interest into the role of citrate in bone development and provided a new hypothesis that osteoblasts were specialized citrate producing cells providing the increased citrate levels necessary for proper bone formation[18]. It is from this rationale that citrate-based materials may enhance bone formation through the presentation of citrate chemistry on the material surface and the release of citrate during the course of material degradation. Our previous studies have shown that citrate-based materials are beneficial for orthopedic applications in that they inherently provide increased citrate levels to the newly forming tissue through material degradation, offer a wide range of controllable material properties, and the ability to be composited with up to 65 wt.-% HA through enhanced bioceramic-polymer interactions, which is a feature not possible with previous orthopedic biomaterials[17,20,22,32].

Although, the functional bio-integration of CABP-HA solid implants has been previously demonstrated to show excellent osteointegration due to their bone-mimicking compositions *in vitro* and *in vivo*, the objective of this study was to compare the efficacy of using bare citric acid-based polymer composite scaffolds to stimulate bone tissue regeneration in a rat calvarial defect model without the use of growth factor supplementation or prior *in vitro* cell seeding[16,17,20,33]. The use of a cranial defect as a means to evaluate bone graft substitutes dates back to more than 100 years when demineralized bovine bone matrix were implanted into the skull of canines[34]. It was later in 1986 that Schmitz and Hollinger established a rat cranial prototype model for osseous nonunions and discontinuity defects[35]. Their results showed that although bone is a dynamic tissue undergoing constant remodeling, its innate ability to heal itself upon injury is largely dependent upon the defect size and location[35,36]. Circular defects created on the rat cranium failed to heal and were filled with fibrous tissue instead of new bone formation over a 3-month period[35–37]. The reduced healing response of the skull was attributed poor blood supply and relative deficiency of bone marrow when compared to other bones[35,38,39]. Unlike typical long bones, there is no primary nutrient artery present rendering the calvarium biologically inert[40]. Instead, blood is primarily supplied by the middle meningeal artery with secondary sources of perfusion being accessory arterioles[41]. These reasons make it especially difficult for even small defects in the skull to spontaneously repair causing many to consider the cranial bone defect as the most severe bone implant test[39].

Although poor blood supply is one of the major reasons for slow bone regeneration in cranial defects, our results show that CABP-HA materials have promoted bone regeneration over time without the use of growth factors or prior cell seeding. Our citric acid based bone

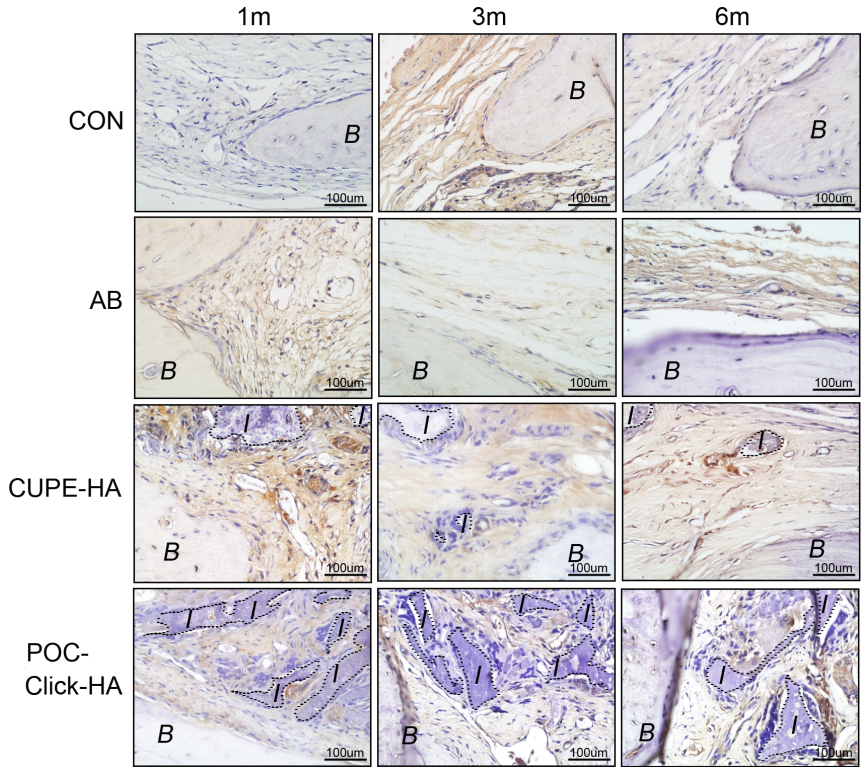

Figure 7 | Vascular endothelial growth factor (VEGF) immunohistochemical stained tissue sections from 4 mm rat calvarial defects treated with crosslinked urethane-doped polyester-hydroxyapatite composite scaffolds (CUPE-HA) and poly (octanediol citrate)-click-hydroxyapatite composite scaffolds (POC-Click-HA) 1, 3, and 6 months of implantation. Both citric acid-based-hydroxyapatite scaffold treated groups (CUPE-HA and POC-Click-HA) displayed larger VEGF-positive areas (brown) in defect sites compared to empty defects (CON) and autologous implant (AB) groups in the same time period (magnification 200×). CON: control group; AB: autogenous bone group; 1 m, 3 m, and 6 m: 1, 3, and 6 months post-surgery, respectively; I: implant I: implant (black dotted lines); B: bone.

substitutes were compared with autogenous bone grafts, which were considered as the gold standard for bone regeneration and osteointegration in clinic due to its inherent ability to provide the ideal biocompatibility and osteogenicity[1,8,42]. Although BMD and Tb.Th values for CABP-HA scaffolds were lower than that of autogenous bone grafts, fibrous-osteotylus formation, a vital marker of intramembranous ossification, was markedly observed in both materials group showing the osteoconductivity of citric acid-based bone substitutes[43]. Alkaline phosphatase (ALP) and osteocalcin (OCN) are considered compelling bio-markers of osteogenesis[44], and our results show the presence ALP positive osteoblasts as well as OCN positive osteoblasts in the defect area of scaffold treated animals. Interestingly, CUPE-HA scaffolds displayed enhanced bone regeneration over POC-Click-HA treated defects in regards to BMD. The increased BMD values may be attributed to the degradation rates of the two materials as previous studies have shown that POC-Click degrades much more rapidly than CUPE-HA[26]. However, the ability of citrate-based materials to stimulate bone regeneration in cranial defects as bare implant materials shows the osteogenic potential of these novel biomaterials.

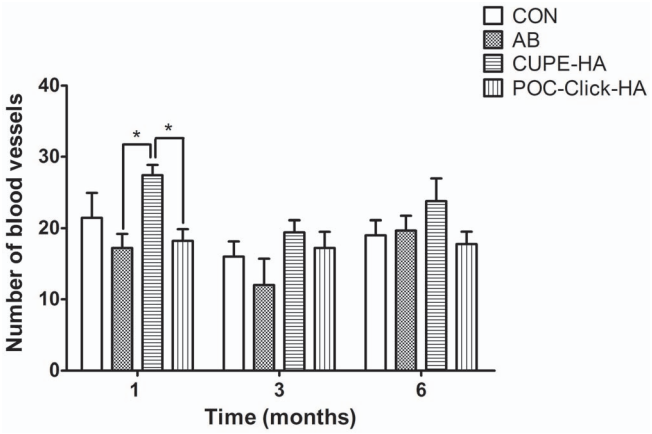

Figure 8 | Number of blood vessels presented in critical sized cranial defects treated with crosslinked urethane-doped polyester-hydroxyapatite composite scaffolds (CUPE-HA), poly (octanediol citrate)-click-hydroxyapatite composite scaffolds (POC-Click-HA), autologous bone (AB), or left empty as a control (CON) 1, 3, and 6 months post-surgery. Data are presented as mean ± SD ($n = 5$). (*$p < 0.05$). CON: negative control group; AB: autogenous bone group.

The lack of a stable and integrated vascular system has been determined to be a significant cause for graft failure[45]. To address this issue, a large number of studies on biomaterials have focused on the bio-graft, which consists of a scaffold, seeded cells, and the release of bio-factors to either induce angiogenesis or recruit host vasculature to impregnate the implanted graft. Vascular endothelial growth factor (VEGF) and bone morphogenetic protein (BMP) are the most common bio-factors applied in tissue engineering and can enhance the regeneration of bone and soft tissue through stimulating angiogenesis and proliferation of seeded cells[46]. To circumvent the long *in vitro* cell culture times and regulatory issues involved with the use of growth factors, recent research in the field has focused on the use of off-the-shelf available acellular systems in which the implanted biomaterial/graft alone can induce tissue regeneration, angiogenesis, and host-cell recruitment to the defect site[47,48]. Surprisingly, a stimulation of soft tissue regeneration and angiogenesis was revealed in animals treated with CABP-HA scaffolds in the early time points. In

our study, increased vessel numbers and a higher level of VEGF expression suggest the development of a satisfactory blood supply during bone and soft tissue regeneration. As blood supply is vital for successful bone grafting, the improved angiogenesis in the defect area after CABP-HA scaffold transplantation indicates that blood supply demands can potentially be remedied through graft transplantation[43,49,50]. In this regard, the two kinds of CABP-HA scaffolds used in this study enhanced VEGF expression in defect area, which is a crucial factor in promoting soft tissue regeneration in the bone defects[51–53]. Although the mechanism of the biomaterial mediated angiogenesis is not well understood at this time, taken together, these results suggest the great potential of citric acid-based hydroxyapatite biomaterials for clinical use.

Conclusions

In conclusion, highly porous disc-shaped citric acid-based polymer hydroxyapatite composite scaffolds were fabricated and used to repair rat calvarial defects. Without incorporating biological growth factors or pre-seeding with stem cells or osteoblastic cells, both POC-Click-HA and CUPE-HA scaffolds displayed satisfactory host responses and osteogenic potential through the stimulation of proximal bone formation and angiogenesis in the repair of calvarial defects. Therefore, citric acid-based polymer hydroxyapatite scaffolds could serve as a promising off-the-shelf implant for the regeneration of bone defects.

1. Giannoudis, P. V., Dinopoulos, H. & Tsiridis, E. Bone substitutes: an update. *Injury* **36 Suppl 3**, S20–27 (2005).
2. Watson, J. T. Overview of biologics. *J. Orthop. Trauma.* **19**, S14–16 (2005).
3. Friedlander, A. H. The physiology, medical management and oral implications of menopause. *J. Am. Dent. Assoc.* **133**, 73–81 (2002).
4. Bauer, T. W. & Muschler, G. F. Bone graft materials. An overview of the basic science. *Clin. Orthop. Relat. R.* **371**, 10–27 (2000).
5. Acarturk, T. O. & Hollinger, J. O. Commercially available demineralized bone matrix compositions to regenerate calvarial critical-sized bone defects. *Plast. Reconstr. Srug.* **118**, 862–873 (2006).
6. Parikh, S. N. Bone graft substitutes: past, present, future. *J. Postgrad. Med* **48**, 142–148 (2002).
7. Carson, J. S. & Bostrom, M. P. Synthetic bone scaffolds and fracture repair. *Injury* **38 Suppl 1**, S33–37 (2007).
8. Damien, C. J. & Parsons, J. R. Bone graft and bone graft substitutes: a review of current technology and applications. *J. Appl. Biomater.* **2**, 187–208 (1991).
9. Lane, J. M., Tomin, E. & Bostrom, M. P. Biosynthetic bone grafting. *Clin. Orthop Relat. R.* **367 Suppl**, S107–117 (1999).
10. Bohner, M. Calcium orthophosphates in medicine: from ceramics to calcium phosphate cements. *Injury* **31 Suppl 4**, 37–47 (2000).
11. Acharya, B. *et al.* Surface immobilization of MEPE peptide onto HA/beta-TCP ceramic particles enhances bone regeneration and remodeling. *J. Biomed. Mater. Res. B.* **100**, 841–849 (2012).
12. Bucholz, R. W. Nonallograft osteoconductive bone graft substitutes. *Clin. Orthop Relat. R.* **395**, 44–52 (2002).
13. Liu, H. & Webster, T. J. Mechanical properties of dispersed ceramic nanoparticles in polymer composites for orthopedic applications. *Int. J. Nanomed.* **5**, 299–313 (2010).
14. Wagoner Johnson, A. J. & Herschler, B. A. A review of the mechanical behavior of CaP and CaP/polymer composites for applications in bone replacement and repair. *Acta. Biomater.* **7**, 16–30 (2011).
15. Zioupos, P., Gresle, M. & Winwood, K. Fatigue strength of human cortical bone: age, physical, and material heterogeneity effects. *J. Biomed. Mater. Res. A.* **86**, 627–636 (2008).
16. Hu, Y. Y., Rawal, A. & Schmidt-Rohr, K. Strongly bound citrate stabilizes the apatite nanocrystals in bone. *P. Natl. Acad. Sci. USA.* **107**, 22425–22429 (2010).
17. Tran, R. T. *et al.* Synthesis and characterization of biomimetic citrate-based biodegradable composites. *J. Biomed. Mater. Res. A.* **102**(8), 2521–32 (2013).
18. Costello, L. C., Franklin, R. B., Reynolds, M. A. & Chellaiah, M. The Important Role of Osteoblasts and Citrate Production in Bone Formation: "Osteoblast Citration" as a New Concept for an Old Relationship. *Open. Bone. J.* **4**, doi:10.2174/1876525401204010027 (2012).
19. Davies, E. *et al.* Citrate bridges between mineral platelets in bone. *P. Natl. Acad. Sci. USA.* **111**, E1354–1363 (2014).
20. Qiu, H., Yang, J., Kodali, P., Koh, J. & Ameer, G. A. A citric acid-based hydroxyapatite composite for orthopedic implants. *Biomaterials* **27**, 5845–5854 (2006).
21. Dey, J. *et al.* Development of biodegradable crosslinked urethane-doped polyester elastomers. *Biomaterials* **29**, 4637–4649 (2008).
22. Yang, J. *et al.* Development of aliphatic biodegradable photoluminescent polymers. *P. Natl. Acad. Sci. USA.* **106**, 10086–10091 (2009).
23. Gyawali, D. *et al.* Fluorescence imaging enabled biodegradable photostable polymeric micelles. *Adv. Healthc. Mater.* **3**, 182–186 (2014).
24. Tran, R. T. *et al.* Synthesis and characterizaion of a biodegradable elastomer featuring a dual crosslinking mechanism. *Soft. Matter.* **6**, 2449–2461 (2010).
25. Gyawali, D., Tran, R. T., Guleserian, K. J., Tang, L. & Yang, J. Citric-acid-derived photo-cross-linked biodegradable elastomers. *J. Biomat. Sci-polym. E.* **21**, 1761–1782 (2010).
26. Guo, J. *et al.* Click Chemistry Plays a Dual Role in Biodegradable Polymer Design. *Adv. Mater.* **26**, 1906–1911 (2013).
27. Dey, J., Xu, H., Nguyen, K. & Yang, J. Crosslinked urethane doped polyester (CUPE) biphasic scaffolds: potential for in vivo vascular tissue engineering. *J. Biomed. Mater. Res. A.* **95A**, 361–370 (2010).
28. Tran, R. T. *et al.* Fabrication and characterization of biomimetic multichanneled crosslinked-urethane doped polyester nerve guides. *J. Biomed. Mater. Res. A.* **102**(8), 2793–804 (2014).
29. Wadajkar, A. S. *et al.* Dual-imaging enabled cancer-targeting nanoparticles. *Adv. Healthc. Mater.* **1**, 450–456 (2012).
30. Sicchieri, L. G., Crippa, G. E., de Oliveira, P. T., Beloti, M. M. & Rosa, A. L. Pore size regulates cell and tissue interactions with PLGA-CaP scaffolds used for bone engineering. *J. Tissue. Eng. Regen M.* **6**, 155–162 (2012).
31. Hartles, R. L. Citrate in Mineralized Tissues. *Adv. Oral. Biol.* **1**, 225–253 (1964).
32. Yang, J., Webb, A. & Ameer, G. Novel citric acid-based biodegradable elastomers for tissue engineering. *Adv. Mater.* **16**, 511–516 (2004).
33. Dickens, F. The citric acid content of animal tissues, with reference to its occurrence in bone and tumour. *Biochem. J.* **35**, 1011–1023 (1941).
34. Senn on the Healing of Aseptic Bone Cavities by Implantation of Antiseptic Decalcified Bone. *Ann. Surg.* **10**, 352–368 (1889).
35. Schmitz, J. P. & Hollinger, J. O. The critical size defect as an experimental model for craniomandibulofacial nonunions. *Clin. Orthop. Relat. R.* **205**, 299–308 (1986).
36. Fini, M. *et al.* The healing of confined critical size cancellous defects in the presence of silk fibroin hydrogel. *Biomaterials* **26**, 3527–3536 (2005).
37. Schmitz, J. P., Schwartz, Z., Hollinger, J. O. & Boyan, B. D. Characterization of rat calvarial nonunion defects. *Acta. Anat.* **138**, 185–192 (1990).
38. Dupoirieux, L., Pourquier, D., Picot, M. C. & Neves, M. Comparative study of three different membranes for guided bone regeneration of rat cranial defects. *Int. J. Oral. Max. Surg.* **30**, 58–62 (2001).
39. Prolo, D. J., Gutierrez, R. V., DeVine, J. S. & Oklund, S. A. Clinical utility of allogeneic skull discs in human craniotomy. *Neurosurgery* **14**, 183–186 (1984).
40. Sirola, K. Regeneration of defects in the calvaria. An experimental study. *Ann. Med. Exp. Biol. Fenn.* **38 (Suppl 2)**, 1–87 (1960).
41. Cutting, C. B., McCarthy, J. G. & Berenstein, A. Blood supply of the upper craniofacial skeleton: the search for composite calvarial bone flaps. *Plastic. Reconstr. Surg.* **74**, 603–610 (1984).
42. Greenwald, A. S. *et al.* Bone-graft substitutes: facts, fictions, and applications. *J. Bone. Joint. Surg. Am.* **83-A Suppl 2 Pt 2**, 98–103 (2001).
43. Liu, X. *et al.* Vascularized bone tissue formation induced by fiber-reinforced scaffolds cultured with osteoblasts and endothelial cells. *Biomed. Res. Int.* **2013**, 854917 (2013).
44. Jane, E. A. *[Mesenchymal Stem Cell and Osteoblast Differentiation] Principles of Bone Biology.* Volume 1. [John P. B., Lawrence G. R., & T, J. M. (3ed.)] [85–108] (Elsevier, Amsterdam, 2008).
45. Willems, W. F., Kremer, T., Friedrich, P. & Bishop, A. T. Surgical Revascularization in Structural Orthotopic Bone Allograft Increases Bone Remodeling. *Clin. Orthop. Relat. R.* **472**(9), 2870–7 (2014).
46. Vunjak-Novakovic, G. *et al.* Dynamic cell seeding of polymer scaffolds for cartilage tissue engineering. *Biotechnol. Progr.* **14**, 193–202 (1998).
47. Ozturk, B. Y. *et al.* The treatment of segmental bone defects in rabbit tibiae with vascular endothelial growth factor (VEGF)-loaded gelatin/hydroxyapatite "cryogel" scaffold. *Eur. J. Orthop. Surg. Tr.* **23**, 767–774 (2013).
48. Han, F. *et al.* Performance of a multilayered small-diameter vascular scaffold dual-loaded with VEGF and PDGF. *Biomaterials* **34**, 7302–7313 (2013).
49. Ahlmann, E., Patzakis, M., Roidis, N., Shepherd, L. & Holtom, P. Comparison of anterior and posterior iliac crest bone grafts in terms of harvest-site morbidity and functional outcomes. *J. Bone. Joint. Surg. Am.* **84-A**, 716–720 (2002).
50. Oakley, M. J., Smith, W. R., Morgan, S. J., Ziran, N. M. & Ziran, B. H. Repetitive posterior iliac crest autograft harvest resulting in an unstable pelvic fracture and infected non-union: case report and review of the literature. *Patient. Saf. Surg.* **1**(1), 6 (2007).
51. Langer, R. & Vacanti, J. P. Tissue engineering. *Science* **260**, 920–926 (1993).
52. Marx, V. Cell culture: a better brew. *Nature* **496**, 253–258 (2013).
53. Griffith, L. G. & Swartz, M. A. Capturing complex 3D tissue physiology in vitro. *Nature. Rev. Mol. Cell. Bio.* **7**, 211–224 (2006).

Acknowledgments

This collaborative work was supported in part by National Natural Sciences Foundation of China (31370987, 31271271 and 31228007), GDHVPS (2011) Program for Changjiang Scholars and Innovative Research Team in University (IRT1142), U.S. National Institutes of

Health (NIH) Awards (NIBIB EB012575, NCI CA182670, NHLBI HL118498), and U.S. National Science Foundation (NSF) Awards (DMR1313553, CMMI 1266116).

Author contributions

D.S., Y.C. and R.T.T. wrote the manuscript; R.T.T. and J.G. made the scaffolds; D.S., S.X. and D.X. conducted animal surgery; C.J., Y.W. and Y.G. prepared figures 1–4; D.S. and Z.Z. prepared figures 5–8; J.Y., D.J. and X.B. were responsible for the research and revised the manuscript. All authors reviewed the manuscript.

Additional information

Supplementary information accompanies this paper at http://www.nature.com/scientificreports

Competing financial interests: The authors declare no competing financial interests.

How to cite this article: Sun, D. *et al.* Citric Acid-based Hydroxyapatite Composite Scaffolds Enhance Calvarial Regeneration. *Sci. Rep.* **4**, 6912; DOI:10.1038/srep06912 (2014).